Static Pressure Measurements in a Hypervelocity Shock Tunnel

GARY H. BOWMAN* AND GRANT W. COON†
NASA Ames Research Center, Moffett Field, Calif.

EXPERIMENTAL difficulties are often encountered when measurements of freestream static pressures are attempted in a hypervelocity shock-driven facility because of the relatively short test time available. The problems may be further compounded by the existence of high-temperature gas in the boundary layer of a test probe, and by the possible carry-over of shock-induced accelerations from the tunnel structure to the measuring element of the transducer. The fact that a high-energy test gas may undergo chemical reactions, either at the surface of a probe or in the surrounding flow field, makes it desirable to minimize the strength of the bow-shock wave of a test probe so as to reduce the resultant chemical disturbance in the flow to as low a value as possible.

The following note describes an experimental technique for measuring stream pressure at the NASA Ames Research Center. The nominal flow properties of the test stream are a static pressure of 0.02 psia, a static temperature of 870°R, and a velocity of 14,500 fps. In actual tests in the shock tunnel, two pressure cells (to be described later) were mounted opposite each other in the wall of a 3-in.-diam, sharp-lipped hollow cylinder as indicated in Fig. 1. The hollow cylinder with supersonic flow inside was chosen to minimize the strength of the leading-edge shock wave and to avoid pressure feedback through the boundary layer from the model support structures. The pressure-cell ports were approximately 0.1 in. deep and were located 4 in. aft of the sharp leading edge. The natural frequency of the cavity was computed to be about 11,000 cps.

The pressure transducers were of the capacitance type, which has been developed at the Ames Research Center. The measuring circuits use 100-kc carrier-amplifier networks designed especially for this application. A further description of this system can be found in Ref. 1. Particular attention was paid to the over-all thickness dimension of the cells in an effort to minimize probe diameter while retaining sufficient internal flow area to prevent choking of the flow through the probe interior. Final cell diameter was 0.27 in., exclusive of the mounting flange and the electrical and reference pressure leads. Cell thickness was about 0.20 in. including the mounting ring.

Each cell had a 0.0005-in.-thick, 48%-Ni-steel diaphragm and was designed to be effective from 0 to 0.1 psia differential pressure. The thermal-expansion coefficient of the 48%-Ni-steel is close to that of the other cell materials. Thus, the cells have been designed to have a minimum response to long-term temperature changes. Nonetheless, the cells could be sensitive to short-term heat pulses, which would cause transient expansion and deflection of the thin diaphragm and result in zero shifts. Consequently, a thermocouple of 0.0005-in.-diam chromel-constantan wires was attached to the face of the cell diaphragm to monitor the temperature of the diaphragm during each test. It was determined from comparison with another cell of the same design, but without the monitor thermocouple, that the presence of the wires on the diaphragm did not affect the pressure or time-response characteristics of the cell.

Extensive prerun bench tests were performed to determine cell sensitivity to short-term heat pulses. Cells were subjected to heat pulses while installed in a small bell jar evacuated to a pressure characteristic of the service environment. The intensity and duration of the heat pulses were controlled

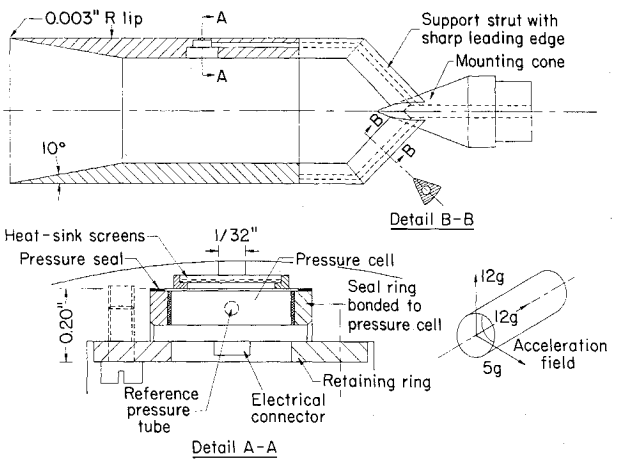

Fig. 1 Static pressure annulus and cell mounting.

by the use of a variable intensity heat lamp in conjunction with a calibrated camera shutter. The cell was subjected to a range of heat pulses; the output signals from the cell and the diaphragm thermocouple were recorded on a dual-trace scope. The data for a particular pressure cell were found to correlate to a single curve, which indicates that the zero-pressure shift is nearly linear with diaphragm temperature change. Figure 2 illustrates this behavior for diaphragm temperature changes up to about 10°F. Note that the maximum zero shift amounts to about 5% of the rated pressure of the transducer.

The amplifiers and 100-kc carrier equipment used during the tests in the shock tunnel were similar to those described in Ref. 1. The output signal was displayed on a high-speed oscillograph. In view of the principle of cell operation, the actual pressure calibration of the cells was performed with the probe mounted in the shock-tunnel test section with the same cables, amplifiers, and oscillograph that were to be used during each test run. The reference pressure was held constant at about 50 μ Hg throughout each run. To prevent severe overloads on the pressure cells, an automatic solenoid valving arrangement was used to vent the reference side of the cells to the test section within milliseconds after the end of the test period. Two layers of 200-mesh bronze screen were posi-

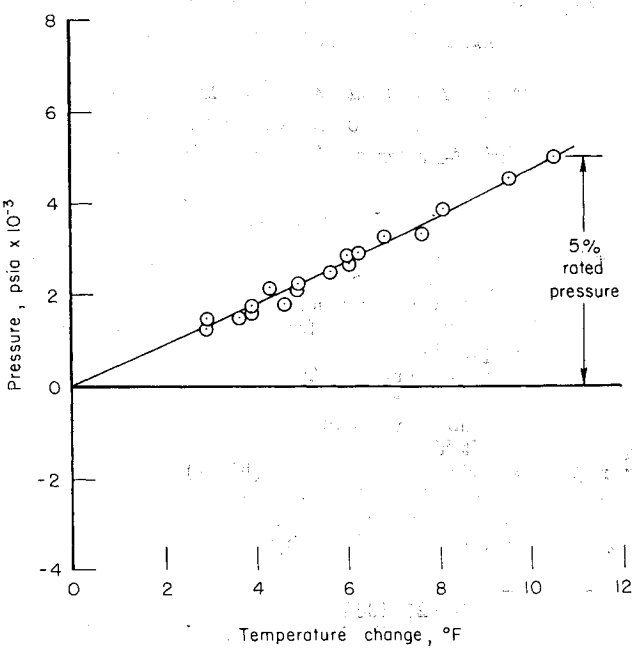

Fig. 2 Pressure indication due to transient heating of cell diaphragm.

Received October 20, 1964.
* Research Scientist, Thermo- and Gas-Dynamics Division.
† Research Scientist, Instrumentation Division.

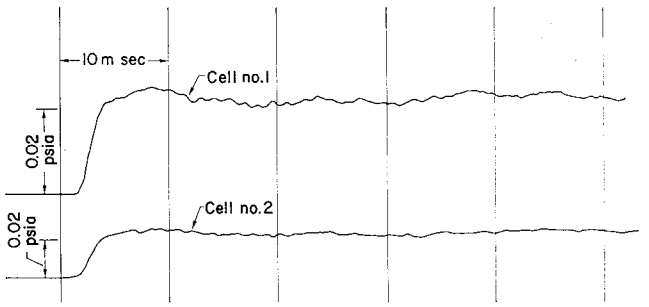

Fig. 3 Typical pressure traces.

tioned ahead of each pressure transducer (see Fig. 1) to act as a heat sink and thus keep the heating of the cell diaphragms to a minimum.

Pressures recorded over a period of 100 msec were on the order of 0.02 psia. A typical oscillograph pressure record is shown in Fig. 3. The time response of the system was limited to that of the galvanometer elements of the oscillograph, which was about 600 cps. The heat-sink screens ahead of the pressure transducers were apparently effective, as evidenced by the fact that the temperature rise of the cell diaphragm was less than 1°F. The resultant error in measurement due to diaphragm heating is not more than about 3% in this instance. The approximate levels of transmitted accelerations in the static-probe support system for this test are shown in Fig. 1. (Previous tests at much higher levels of shock-induced accelerations have shown that these transducers are relatively insensitive to "g" loads.) Pictures taken of the model during the test runs offer evidence that the flow through the probe interior was supersonic. The accuracy of the measured pressures is believed to be limited to the accuracy in reading the oscillograph traces, which is of the order of 5%.

Reference

[1] Dimeff, J., "A survey of new developments in pressure measuring techniques in the NACA," AGARD Conference, London (March 24–28, 1958).

Hypersonic Stability Derivatives of Blunted Slender Cones

Otto Walchner* and James T. Clay†
Aerospace Research Laboratories, Wright-Patterson Air Force Base, Ohio

Nomenclature

$d = 2R$	=	base diameter
$d_N = 2r_N$	=	nose diameter
dS	=	cone surface element (Fig. 1)
l	=	length, measured from the shoulder of the nose
M	=	pitching moment
n	=	pressure ratio $C_p/2\theta_c^2$
p_s	=	surface pressure
p_∞	=	ambient pressure
q	=	pitching velocity
r, x, ϕ	=	cylindrical coordinates (Fig. 1)
Re_l	=	Reynolds number based on l
V	=	velocity vector of c.g.
V_e	=	effective local velocity
V_N	=	velocity component perpendicular to the cone surface
α	=	static angle of attack
α_e	=	effective local angle of attack
θ_c	=	cone half angle
ρ	=	ambient density
ξ	=	nose bluntness ratio r_N/R
C_p	=	pressure coefficient $(p_s - p_\infty)/(\rho/2)V^2$
C_m	=	$M/(\rho/2)V^2R^2\pi l$ pitching moment coefficient
C_{m_α}	=	$\partial C_m/\partial\alpha$ static stability derivative
C_{m_q}	=	$\partial C_m/\partial(ql/V)$ damping derivative
C	=	$[\theta_c(1-\xi)/2\xi]^{1/2}$ correlation parameter

Received October 21, 1964

* Research Aerospace Engineer, Hypersonic Research Laboratory.

† Research Aerospace Engineer, Hypersonic Research Laboratory; also Captain, U. S. Air Force. Member AIAA.

Introduction

THE Newtonian impact theory with the pressure coefficient $C_p = 2(V_N/V)^2$ fails to predict the pressure distribution over slender, blunted cones and, therefore, must fail to predict the stability derivatives C_{m_α} and C_{m_q}. Thus, the occasionally observed agreement of one or the other derivative with the Newtonian prediction is believed to be accidental.

In the following, a semiempirical theory is presented based on Cheng's[1] analysis of slender blunted cones at zero angle of attack, while the tangent cone approximation is used to account for angle-of-attack effects. Quasi steady-state conditions are assumed to be valid.

Analysis

From Fig. 1 it can be seen that a cone element at the station x produces the differential pitching moment coefficient about the c.g.:

$$dC_m = \frac{2}{R^2\pi l}\int_{\phi=-\pi/2}^{\phi=+\pi/2}[r\sin\phi\,\sin\theta_c + (x - x_{c.g.})\cos\theta_c\sin\phi]C_p\,dS$$

where $dS = rd\phi dx/\cos\theta_c$. Substituting geometric relations from Fig. 1 and expressing the nose bluntness ratio by $\xi = r_N/R$, we obtain

$$dC_m = \frac{2}{\pi\tan\theta_c}\left[\frac{x}{l}(1-\xi\cos\theta_c)^2 + \xi\cos\theta_c(1-\xi\cos\theta_c)\right]\times\left[\frac{x}{l}(1+\tan^2\theta_c) - \frac{x_{c.g.}}{l} + \frac{\xi\cos\theta_c}{1-\xi\cos\theta_c}\tan^2\theta_c\right]\times d\left(\frac{x}{l}\right)\int_{-\pi/2}^{+\pi/2}C_p\sin\phi d\phi \quad (1)$$

Now, for slender cones with moderate nose bluntness

$$\cos\theta_c \sim 1 \qquad \tan\theta_c \sim \theta_c \qquad \frac{\xi}{1-\xi}\tan^2\theta_c \ll 1$$

$$\tan^2\theta_c \ll 1$$

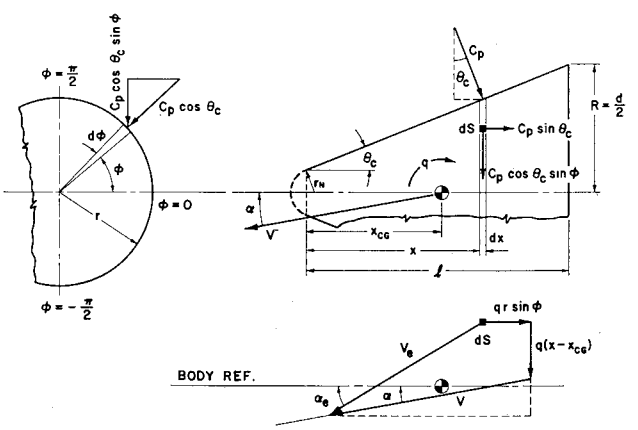

Fig. 1 Geometry of the investigated shape, pressure and velocity components for the surface element dS.